

TgCep250 is dynamically processed through the division cycle and is essential for structural integrity of the *Toxoplasma* centrosome

Chun-Ti Chen* and Marc-Jan Gubbels*

Department of Biology, Boston College, Chestnut Hill, MA 02467

ABSTRACT The apicomplexan centrosome has a unique bipartite structure comprising an inner and outer core responsible for the nuclear cycle (mitosis) and budding cycles (cytokinesis), respectively. Although these two cores are always associated, they function independently to facilitate polyploid intermediates in the production of many progeny per replication round. Here, we describe the function of a large coiled-coil protein in *Toxoplasma gondii*, TgCep250, in connecting the two centrosomal cores and promoting their structural integrity. Throughout the cell cycle, TgCep250 localizes to the inner core but, associated with proteolytic processing, is also present on the outer core during the onset of cell division. In the absence of TgCep250, stray centrosome inner and outer core foci were observed. The detachment between centrosomal inner and outer cores was found in only one of the centrosomes during cell division, indicating distinct states of mother and daughter centrosomes. In mammals, Cep250 processing is required for centrosomal splitting and is mediated by Nek phosphorylation. However, we show that neither the nonoverlapping spatiotemporal localization of TgNek1 and TgCep250 nor the distinct phenotypes upon their respective depletion support conservation of this mechanism in *Toxoplasma*. In conclusion, TgCep250 has a tethering function tailored to the unique bipartite centrosome in the Apicomplexa.

Monitoring Editor

Fred Chang
University of California,
San Francisco

Received: Oct 1, 2018

Revised: Jan 24, 2019

Accepted: Mar 5, 2019

INTRODUCTION

The phylum Apicomplexa consists almost exclusively of obligate intracellular parasites that have significant impact on public health. Among these single-celled organisms, *Toxoplasma gondii* is one of the most successful zoonotic pathogens that can be transmitted and replicate in many different host species. *Toxoplasma gondii* has developed flexible replication strategies allowing efficient survival in distinct tissue types. Tachyzoites are the acute replication form of

T. gondii and are responsible for most of the clinical burden in infected individuals. They undergo a binary replication mode termed endodyogeny, wherein two daughter cells assemble within and emerge from the mother cell. The cell cycle follows the sequence of G1, S, and M phases, but the G2 phase is absent or too short to be detected (Gubbels *et al.*, 2008) and is driven by a set of unconventional cyclin-dependent kinase-related kinases and cyclins (Alvarez and Suvorova, 2017). Mitosis is (semi)closed and spatiotemporally coordinated with cytokinesis, as these two events occur concomitantly. The 13 chromosomes are clustered at the centromeric region throughout the cell cycle at the “centrocone,” a unique membranous structure that houses the spindle microtubule during mitosis (Brooks *et al.*, 2011). The tight organization of chromosomes is thought to ensure that each daughter cell receives a full set of genetic material when the parasite undergoes a more complex division cycle in other developmental stages (Francia and Striepen, 2014). In its definitive feline host, endopolygeny consists of several rounds of DNA synthesis and mitosis in the same cytoplasmic mass followed by synchronized cytokinesis in accordance with the last round of mitosis, producing 8–16 uninucleated progeny per replication cycle (Ferguson *et al.*, 1974).

This article was published online ahead of print in MBc in Press (<http://www.molbiolcell.org/cgi/doi/10.1091/mbc.E18-10-0608>) on March 13, 2019.

*Address correspondence to: Chun-Ti Chen (chuntid.chen@gmail.com) or Marc-Jan Gubbels (gubbelsj@bc.edu).

Abbreviations used: ATc, anhydrotetracycline; DAPI, 4',6'-diamidino-2-phenylindole; HA, hemagglutinin; IFA, immunofluorescence assay; ISP1, IMC-subcompartment protein 1; LIC, ligation-independent cloning; PCM, peripheral centrosomal matrix; SFA, striated fiber assemblin; SIM, structured illumination microscopy; YFP, yellow fluorescent protein.

© 2019 Chen and Gubbels. This article is distributed by The American Society for Cell Biology under license from the author(s). Two months after publication it is available to the public under an Attribution–Noncommercial–Share Alike 3.0 Unported Creative Commons License (<http://creativecommons.org/licenses/by-nc-sa/3.0>).

“ASCB®,” “The American Society for Cell Biology®,” and “Molecular Biology of the Cell®” are registered trademarks of The American Society for Cell Biology.

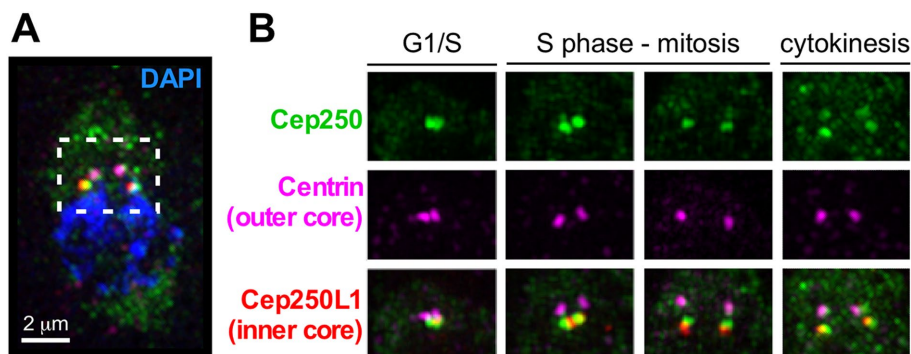


FIGURE 1: Dynamic localization of TgCep250 throughout the cell cycle. (A) IFA of TgCep250-YFP parasites costained with α -GFP (Cep250, shown in green), α -Centrin (centrosomal outer core marker, shown in magenta), α -HA (centrosomal inner core marker shown in red), and DAPI (in blue). Images acquired by superresolution microscopy (SIM). (B) Single-color panels show dynamic localization of TgCep250-YFP during asexual division cycle, essentially as previously reported (Suvorova *et al.*, 2015). Cell cycle stages as indicated.

The *Toxoplasma* centrosome is divergent from mammalian cells in architecture and composition. For example, the centrioles are composed of nine singlet microtubules, smaller in size than mammalian centrioles, and the centriole pair is arranged in parallel rather than perpendicular (Francia and Striepen, 2014). Orthologues of many key components in the mammalian centrosome cannot be found in the *Toxoplasma* genome (Morlon-Guyot *et al.*, 2017). Even without canonical protein orthologues, recent studies have shown that a group of coiled-coil proteins localize to the centrosome and support proper karyokinesis and cytokinesis (Suvorova *et al.*, 2015; Courjol and Gissot, 2018). This work identified a distinctive architecture of two centrosomal cores: the outer core (distal to the nucleus) and the inner core (proximal to the nucleus). Independent activation of the inner and outer cores has been proposed as the mechanism underlying the uncoupling of S/M from daughter budding during polyploid intermediate stages across apicomplexan division modes, including endopolygony in *Toxoplasma* and schizogony in the malaria-causing *Plasmodium* spp. (Chen and Gubbels, 2015; Suvorova *et al.*, 2015).

The *Toxoplasma* centrosome is the key organelle coordinating mitotic and cytokinetic rounds. The centrosome resides at the apical end of the nucleus during interphase and remains closely associated with a specialized nuclear envelope fold, the centrocone, which houses the spindle microtubules during mitosis (Gubbels *et al.*, 2006). The centrosome also plays a critical role in partitioning the single-copy Golgi apparatus and the chloroplast-like organelle, the apicoplast, during cell division (Nishi *et al.*, 2008). Late in G1, the centrosome rotates to the distal end of the nucleus, where it duplicates and then returns to the proximal end (Chen *et al.*, 2015). At this point, the spindle microtubules assemble and are stabilized within the centrocone, whereas subsequently the centrosome serves as a scaffold for assembly of daughter cell cytoskeletal components (Anderson-White *et al.*, 2012). In mitosis, a striated fiber assemblin (SFA) protein emanates from the centrosome and connects the daughter apical conoid to the centrocone. SFA polymerization is thought to maintain the stoichiometric count of daughter cells and replicating genomic materials. In SFA-depleted cells, cell division is completely disrupted (Francia *et al.*, 2012). Little is known about centrosome biogenesis or regulation during these tightly regulated events in *Toxoplasma*. Although orthologues in charge of new centriolar biogenesis, Polo-like kinase PLK4 and its substrate STIL/Ana2/SAS5, are absent from the *Toxoplasma* genome, previous work has shown that a conserved NIMA-kinase, TgNek1, is required for centrosomal splitting (Chen and Gubbels, 2013), and a

TgMAPK-L1 plays a role in inhibiting centrosomal overduplication (Suvorova *et al.*, 2015). However, exactly what aspects of the centrosome these kinases act upon and what their substrates are remains unclear.

Here, we asked whether the previously described TgCep250 (Suvorova *et al.*, 2015) could be the substrate of TgNek1 required for centrosomal splitting orthologous to the human HsNek2-C-NAP1/Cep250 relationship in centrosome splitting (Agircan *et al.*, 2014). In our interpretation of the data, this hypothesis is rejected, but it is instead revealed that TgCep250 is required to connect the inner core with the outer core and to maintain overall centrosomal integrity. Moreover, these data represent the first experimental observation directly hinting at a differential status of mother versus daughter

centrosome in the Apicomplexa. In conclusion, although TgCep250 is not the critical TgNek1 substrate, its function in keeping centrosomal complexes connected appears to be parallel to the role of human C-NAP1/Cep250 in managing structural connections in the centrosome.

RESULTS

TgCep250 has a dynamic localization and is associated with proteolysis

To start charting the function of the previously reported *Toxoplasma* centrosomal protein TgCep250 (TGGT1_212880) (Suvorova *et al.*, 2015), we first confirmed the subcellular localization of TgCep250 throughout the parasite's tachyzoite division cycle. TgCep250 was tagged endogenously with a C-terminal yellow fluorescent protein (YFP) tag (Huynh and Carruthers, 2009), and the TgCep250-YFP parasite line was transfected with a fosmid expressing TgCep250L1-hemagglutinin (HA) as an inner core centrosomal marker (Suvorova *et al.*, 2015). During the G1 phase of the cell cycle, TgCep250-YFP is closely associated with the centrosomal inner core (highlighted by TgCep250L1), whereas during cytokinesis, we observed four TgCep250-YFP foci (Figure 1). The upper two foci were in close apposition to the outer core, and these results are in agreement with previous observations (Suvorova *et al.*, 2015).

To dissect the function of TgCep250, we generated a conditional knockdown line (TgCep250-cKD) using a tetracycline-regulatable promoter. Simultaneously, we inserted a single-Myc tag at the N-terminus of the gene (Figure 2A). Correct integration of the construct through single homologous recombination was validated by PCR (Figure 2B). In the presence of anhydrotetracycline (ATc), Myc-TgCep250 protein becomes undetectable within 6 h of incubation by immunofluorescence assay (IFA) and Western blot (Figure 2, C and D). Interestingly, the N-terminal Myc-tagged TgCep250 only formed two foci colocalizing with outer core marker α -Centrin throughout the cell cycle. This suggested that the placement of the tag on TgCep250 either alters the subcellular localization or that proteolytic processing is associated with this differential localization pattern. To test this hypothesis, we added a C-terminal 3xTy tag to the Myc-TgCep250-cKD locus (Figure 3A) and analyzed TgCep250-3xTy by IFA and Western blot. As shown in Figure 3, B and C, C-terminally 3xTy-tagged TgCep250 forms four foci like TgCep250-YFP. Moreover, we observed multiple protein bands smaller than the full-length protein on the blot using α -Ty antibody (Figure 3C; note that full-length TgCep250 is a large coil-coiled protein with a molecular weight

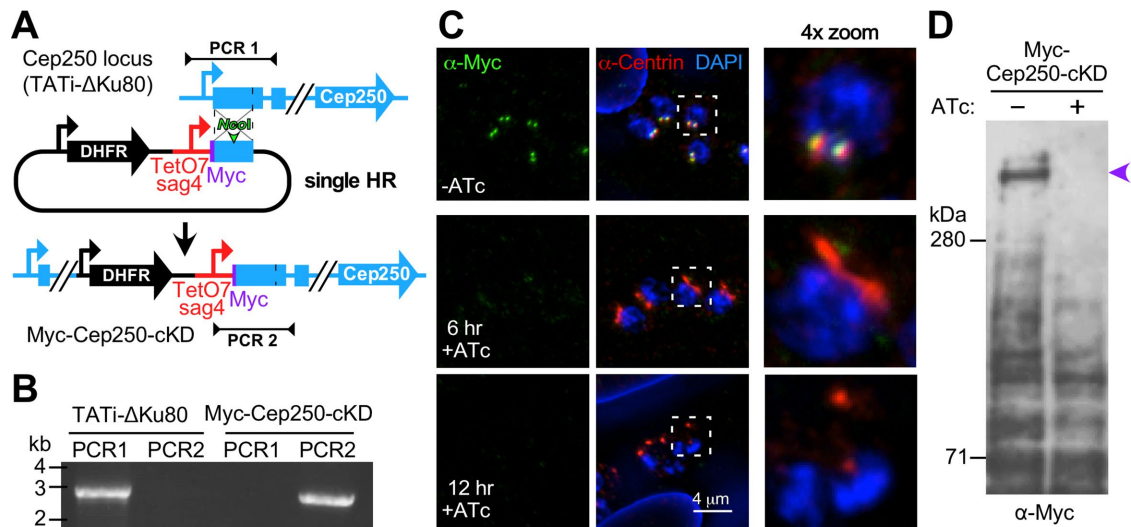


FIGURE 2: Generation and validation of a TgCep250-cKD line. (A) Schematic representation of TgCep250 conditional knockdown (cKD) construction by single homologous recombination. (B) PCR validation using TATI-ΔKu80 (parent) and Myc-TgCep250-cKD genomic DNA as templates. Primer pairs as indicated in A. (C) IFA using α -Myc and α -Centrin showed that the Myc-tagged TgCep250 is depleted within 6-h incubation of ATc. Boxed areas are magnified in the 4 \times zoom panels. (D) Western blot using α -Myc showed that the protein expression level is down-regulated in the presence of ATc. The purple arrowhead marks the full-length Cep250 protein (note that TgCep250 has a predicted molecular weight of 762 kDa); the smaller bands present in both the -ATc and +ATc samples are considered aspecific and serve as loading controls.

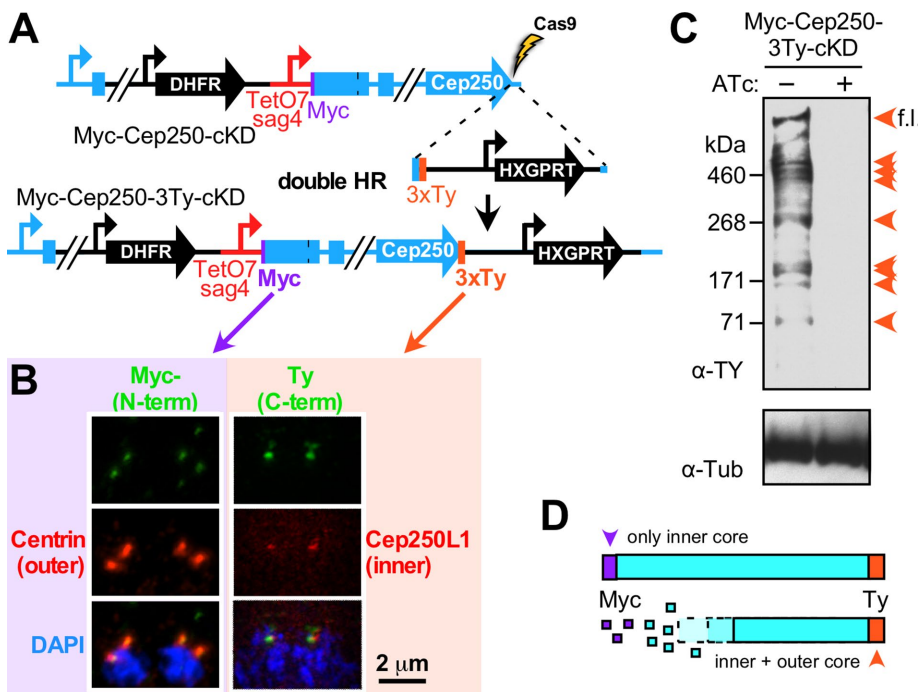


FIGURE 3: Differential localization of TgCep250 is regulated by proteolysis. (A) Schematic representation of Myc-TgCep250-3xTy-cKD construction using CRISPR/Cas9. (B) Myc-TgCep250-cKD localized only to the outer core (stained with α -Myc and α -Centrin) and TgCep250-3xTy localized to both inner and outer core (stained with α -Ty and α -HA on endogenously tagged TgCep250L1-HA as inner core marker). Left, conventional wide-field microscopy; right, superresolution (SIM) microscopy. (C) Multiple protein bands were detected in Western blot using α -Ty antibody suggestive of extensive proteolytic processing. α -Tubulin antiserum (12G10) was used as a loading control. Orange arrowheads mark the specifically detected TgCep250 protein fragments. (D) Schematic interpretation of Western blot and IFA data representing the relationship between TgCep250 proteolysis and subcellular localization.

predicted to be 762 kDa). Thus, these data support the notion that only full-length TgCep250 localizes to the outer core (during the onset of cytokinesis), and a truncated version of TgCep250 localizes to the inner core (throughout all cell cycle stages; Figure 3, B and D). In line with this hypothesis, we only detected a single band on the Western blot, which is consistent with the full-length protein using α -Myc antibody (Figure 2D).

TgCep250 is essential and links the centrosomal inner and outer cores

Next, we probed the function of TgCep250 with a series of experiments using the TgCep250-cKD parasite line. In the presence of ATc, TgCep250-cKD parasites failed to form plaques, suggesting TgCep250 is essential for parasite survival (Figure 4A). Phenotypic analysis by IFA showed that, in the absence of TgCep250, the nucleus failed to partition to the daughter cells (Figure 4B, white arrow), and as a result, anuclear parasites were observed (Figure 4B, white arrowheads). After 24 h of ATc induction, ~90% of all vacuoles harbored a parasite with a mislocalized nucleus (Figure 4C). Furthermore, we noticed that the stoichiometric balance of 1:1 daughter to (outer)centrosome count was also disrupted, resulting in multiple Centrin foci being accumulated in a single cell boundary, as outlined by IMC3, a cortical cytoskeleton marker (Figure 4B, double arrowhead). To examine

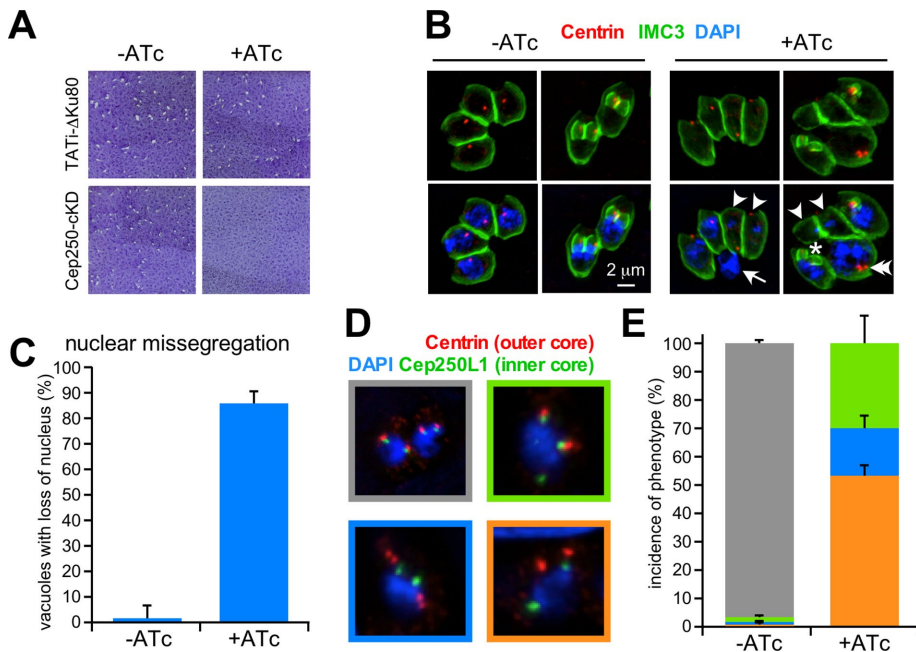


FIGURE 4: Loss of TgCep250 causes lethal centrosomal defects. (A) Plaque assay of TgCep250-cKD and the TATI-ΔKu80 parent line ± ATc for 7 d shows that TgCep250 is essential. (B) IFA of TgCep250-cKD stained with α-Centrin (in red) and α-IMC3 (in green) ± ATc for 24 h. Arrowheads mark parasites with nuclear loss; arrow marks a nucleus outside a parasite; double arrowhead marks a parasite with two nuclei and three outer cores; asterisk marks a parasite with daughter buds out of sync with the rest of the vacuole. (C) Quantification of nuclear loss as shown in B. Vacuoles were scored for loss of at least one nucleus from the present parasites. At least 100 vacuoles (harboring four or more parasites) per experiment and condition were counted; error bars represent SD from three independent experiments. (D) TgCep250-cKD parasites coexpressing TgCep250L1-HA were stained with α-Centrin (in red) and α-HA (in green) marking the outer and inner cores, respectively. Images are representative of observed phenotypes; gray box: control wild-type nuclei displaying duplicated centrosomes; green box: stray inner core complex in presence of two normal appearing inner/outer pairs; blue box: outer core duplication independent of inner core duplication; orange box: complete detachment of inner and outer cores. (E) Quantification of defective centrosomal phenotypes; bar colors match the colored boxes in D. At least 100 nuclei with a duplicated centrosome pair per experiment and condition were counted; error bars represent SD from three independent experiments.

the nuclear partitioning defect in more detail, we used different sets of antibodies to analyze TgCep250-depleted parasites. We defined three different classes of centrosomal defects in TgCep250-depleted cells using centrosomal inner (TgCep250L1) and outer core (Centrin) markers (Figure 4, D and E). Detachment of the inner core from the outer core was observed in the majority of mitotic, mutant parasites (marked in orange). Furthermore, we observed parasites in which the outer core split into two foci, while only two inner cores were present, suggestive of the parasite undergoing an additional replication cycle (marked in blue; 10% of the mitotic parasites). Finally, nearly 35% of the mitotic parasites displayed stray inner core foci (marked in green). Detachment of inner and outer cores likely results in the nuclear-partitioning defect observed in Figure 4B, which therefore is a secondary defect. An additional observation is that detachment of inner and outer cores occurred in most instances on only one of the two centrosomes. The most logical explanation is that the detached inner and outer core pair represents the daughter centrosome and the intact pair represents the mother centrosome (Bornens and Gonczy, 2014). In this scenario, during centrosomal biogenesis, TgCep250 cannot be incorporated into the newly formed daughter centrosome, resulting in disconnection of the inner and outer cores.

we costained the parasite with inner core (TgCep250L1) and kinetochore (TgNdc80) markers. We observed multiple TgCep250L1 foci, of which one typically still colocalized with the kinetochore, and one was detached from both the nucleus (Figure 5C). Quantification of this phenotype confirmed this in ~50% of the vacuoles in the earliest division round of phenotype induction (Figure 5D). Consistent with the observation in Figure 4, we noticed only a small fraction of parasites in which both inner cores had fragmented, further supporting the notion that Cep250 depletion does not affect the mother centrosome.

Next, we asked whether the outer core retained functionality. We first used IMC-subcompartment protein 1 (ISP1) as a marker for early daughter formation near the centrosome (Beck *et al.*, 2010). As shown in Figure 5E, α-ISP1 signal was detected surrounding the outer core in the presence and absence of ATc, even when the outer core was detached from the inner core (Figure 5E, 4x zoom, asterisk). As a second marker for daughter bud development, we used the SFA protein, which connects the centrosome with daughter bud (Francia *et al.*, 2012) in combination with Centrin (outer core), TgCep250L1 (inner core), and TgNdc80 (kinetochore). We observed SFA fibers emanating from the outer core, which is again consistent with full functionality of the detached outer core (Figure 5F). As

However, the TgCep250 in the mother centrosome is stably incorporated, thereby maintaining inner and outer core adhesion in this centrosome. Indeed probing Myc-TgCep250-3xTy-cKD parasites with Ty antiserum confirmed that Cep250 was still present in the normal-looking, mother centrosome, whereas it was either strongly depleted or undetectable in the daughter centrosome (Supplemental Figure S1).

Disconnected inner and outer cores retain their function

The anuclear phenotype observed in TgCep250-cKD parasites was very similar to the anuclear daughters observed in parasites depleted in kinetochore component TgNuf2 (Farrell and Gubbels, 2014). We tested how these two observations relate to each other and whether the inner core is still functional when it is separated from the outer core. IFA assays using mitotic markers revealed the interactions between centrosomal outer core (α-Centrin), the kinetochore (α-TgNdc80 or α-TgNuf2) (Farrell and Gubbels, 2014), and the spindle microtubules (EB1-YFP or α-TgEB1) (Chen *et al.*, 2015) (Figure 5A). In the absence of TgCep250, both kinetochore complex and spindle microtubules became detached from the centrosomal outer core (Figure 5A, white arrowhead). Using an EB1 and Centrin costain, we determined that, while the spindle retained its normal morphology, the disconnect from the outer core occurred in roughly 50% of the vacuoles going through the first division following phenotype induction (Figure 5B). To determine whether TgCep250 plays a role in interaction between the inner core and the kinetochore,

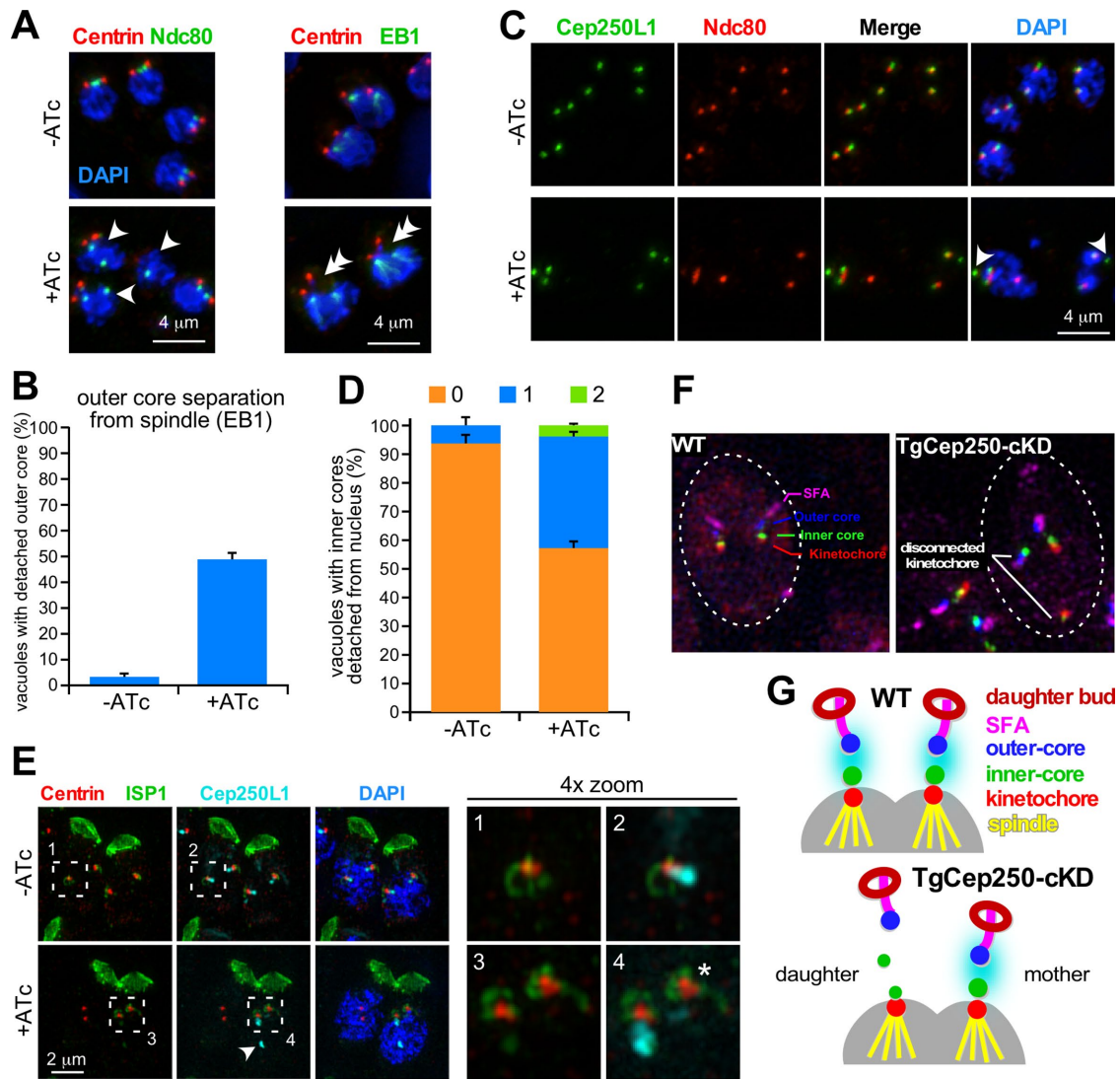


FIGURE 5: The inner and outer cores remain functional upon dissociation in TgCep250-depleted parasites. Assessment of inner core (A–D) and outer core (E and F) function in TgCep250-depleted parasites. (A) IFA of TgCep250-cKD \pm ATc for 18 h stained with α -Centrin (outer core; red) and costained with either α -TgNdc80 (kinetochore; green; left) or coexpression of TgEB1-YFP (spindle microtubules; green; right). Arrowheads mark nuclei displaying loss of outer core association with the kinetochore; double arrowheads mark nuclei displaying loss of outer core association with the spindle. No spindle or kinetochore defects were observed, indicating the inner core is fully functional. (B) Quantitation of the Centrin and EB1 staining represented in A using TgCentrin1 and TgEB1 antisera on TgCep250-cKD parasites induced \pm ATc for 18 h. The incidence of loss of the connection between these structures in at least one nucleus per vacuole was scored. At least 100 nuclei with a spindle EB1 signal per experiment and condition were counted; error bars represent SD from three independent experiments. (C) IFA of TgCep250-cKD \pm ATc for 18 h expressing TgCep250L1-HA (inner core: α -HA; green) and costained with α -TgNdc80 (kinetochore; red) showed that the interaction between the kinetochore and inner core centrosome remains intact in the absence of TgCep250. (D) Quantitation of the phenotype observed in C using HA and TgNuf2 antisera on TgCep250-cKD parasites induced \pm ATc for 18 h. The incidence of loss of the connection between these structures in at least one nucleus per vacuole was scored for loss of no, one, or two lost connections. Also scored, but not plotted, were incidences of kinetochores outside the nucleus in absence ($1.16 \pm 0.48\%$) and presence of ATc ($0.76 \pm 0.67\%$). At least 100 nuclei with a duplicated kinetochore per experiment and condition were counted; error bars represent SD from three independent experiments. (E) Superresolution (SIM) IFA of TgCep250-cKD \pm ATc coexpressing TgCep250L1-HA stained with α -ISP1 (green: early daughter scaffold marker), α -Centrin (red: outer core), and α -HA (cyan: inner core). Numbered, boxed areas are magnified on the right. Note that outer cores are normally associated with daughter scaffolds (asterisk), even if the inner core connection is lost (arrowhead). (F) Superresolution (SIM) IFA of TgCep250-cKD coexpressing TgCep250L1-HA stained with α -HA (green: inner core), α -Centrin (blue: outer core), α -TgSFA (magenta: daughter tether), and α -TgNdc80 (red: kinetochore). Dotted lines outline parasites. (G) Summarizing schematic representation of data interpretation illustrating that inner and outer cores function normally upon their separation due to TgCep250 depletion.

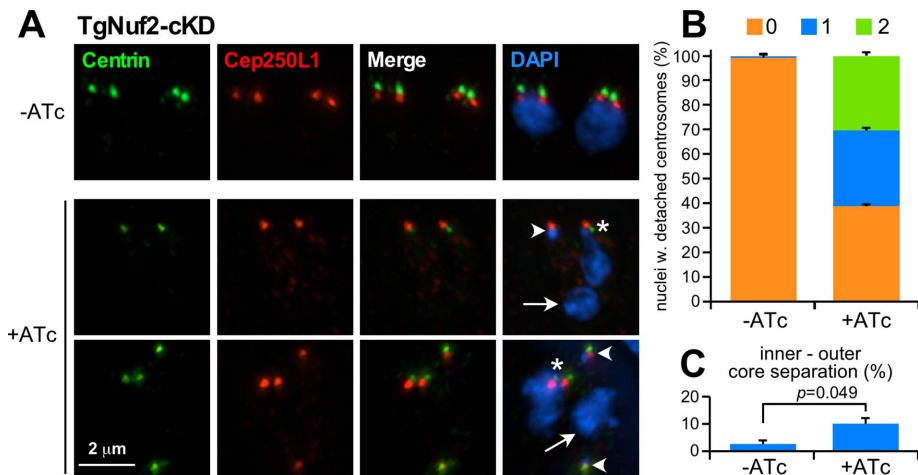


FIGURE 6: The kinetochore is required to anchor centrosomal cores to the nuclear periphery. (A) TgNuf2-cKD parasites treated \pm ATc for 18 h stained with centrosomal outer core (α -Centrin, in green) and inner core (TgCep250L1-HA; α -HA, in red) markers. Asterisks mark intact nucleus-centrosome connections; arrowheads mark intact inner and outer core pairs strayed from the nucleus (the associated small DAPI spot is the plastid genome); arrows mark missegregated nuclei. (B) Quantification of data in A. At least 100 vacuoles with a duplicated centrosome pair in each parasite were counted per experiment and condition and scored for loss of no, one, or two centrosomes per nucleus (maximum observed per vacuole was scored); error bars represent SD from three independent experiments. (C) The centrosomes counted in B were further differentiated for inner and outer core separation; error bars represent SD from the same three independent experiments as in B. Statistical analysis by two-tailed t test.

summarized in Figure 5G, although we saw inner core fragmentation in the absence of Cep250, the inner core fragment retained at the nucleus remained associated with the kinetochore and was fully functional in spindle formation, whereas the detached outer core was still fully able to nucleate daughter scaffolds.

TgNuf2 anchors the centrosome to the nuclear periphery

To further dissect the association between the inner core and the kinetochore, we expressed the inner core marker TgCep250L1 in a kinetochore-depleted parasite line, TgNuf2-cKD (Farrell and Gubbels, 2014). It has been reported that, in the absence of TgNuf2, the association between the (outer)centrosome and spindle pole was abolished and that the (outer)centrosome pulled away from the nucleus (Farrell and Gubbels, 2014). With the inner core marker in the Nuf2-cKD background, we observed that the connection between the inner and outer core remained intact and that the whole centrosome dissociated from the nucleus (Figure 6A). We observed an approximately equal number of parasites in which either one or both centrosomes were dissociated (Figure 6B), which suggests there is not a mother and daughter distinction in this scenario. Although the majority of centrosomes did not fragment, we observed a statically relevant increase in inner and outer core dissociation from 2.4 to 10% (Figure 6C).

TgNek1 promotes separation of only the outer cores

It has been shown that a *Toxoplasma* orthologue of NIMA kinases, TgNek1, facilitates centrosomal splitting in tachyzoites (Chen and Gubbels, 2013). To dissect the regulation of centrosomal core splitting in a TgNek1-depleted background, we constructed a conditional knockdown line of TgNek1 (TgNek1-cKD) (Supplemental Figure S2A). Plaque assays showed that, in the presence of ATc, TgNek1-cKD parasites display a severe growth defect (Supplemental Figure S2B) consistent with the temperature-sensitive TgNek1 phenotype

previously reported (Chen and Gubbels, 2013). Moreover, IFA with α -TgNek1 confirmed that TgNek1 expression is depleted in the presence of ATc (Supplemental Figure S2C). Interestingly, upon depletion of TgNek1, the duplicated outer cores remain connected, whereas the inner cores separate along with the kinetochores (Figure 7A). The distance between separated kinetochores in TgNek1-cKD and wild-type parasites is comparable, which in turn is comparable with previously reported distances (Suvorova et al., 2015). Quantification of kinetochore separation relative to outer core separation revealed that this is a very strong phenotype (Figure 7, B–D) and indicates that the spindle is able to separate the kinetochores, along with the inner cores, when outer core splitting is blocked.

DISCUSSION

In mammalian cells, duplicated centrosomes are tethered together by a fiber complex composed of C-NAP1/Cep250 (Fry et al., 1998), rootletin (Bahe et al., 2005), and LRRC45 (He et al., 2013). Phosphorylation of C-NAP1/Cep250 by NIMA kinase Nek2 promotes degradation of C-NAP1/Cep250 and results in splitting of the linked centrosomes (Fry et al., 1998). Reciprocal BLAST analysis revealed a family of *Toxoplasma* proteins displaying features of the C-NAP1/Cep250 and rootletin orthologues, of which two localize to the centrosomes: TgCep250 (763 kDa) and TgCep250L1 (296 kDa) (Suvorova et al., 2015; Morlon-Guyot et al., 2017). Because TgCep250 showed dynamic changes associated with centrosomal replication (Suvorova et al., 2015), we asked whether regulatory and/or structural features might be conserved as well between mammals and *Toxoplasma*.

We showed that the functional orthologue of human Nek2 in *Toxoplasma*, TgNek1, is essential for outer core but not inner core splitting (Figures 7 and 8). This observation implies that the substrate of TgNek1 only tethers the outer core and the mechanism that physically separates the inner and outer core is different. Both TgNek1 and TgCep250 are closely associated with the centrosomal outer core; however, their timing is different. TgNek1 is only transiently recruited to the centrosome in G1/S-phase transition and disappears after the cell cycle progresses into mitosis (Chen and Gubbels, 2013), which is just when TgCep250 shows up in the outer core (summarized in Figure 8). Thus, although we cannot formally exclude the possibility that TgCep250 is a TgNek1 substrate, the proteolytic event of TgCep250 that leads to both inner and outer core localization is likely independent from TgNek1 activity, because TgNek1 is already absent from the centrosome during cytokinesis. Phenotypic analysis of the TgCep250-cKD and TgNek1-cKD phenotypes also showed different cell cycle defects, indicating the roles of TgCep250 and TgNek1 are functionally distinct (Figure 8). It is worth noticing that TgCep250 is phosphorylated at Ser-252 in whole-organism phosphoproteome data (Treec et al., 2011). However, the function of this TgCep250 phosphorylation and the kinase that phosphorylates it remain to be determined. HsNek2 phosphorylation of HsCep250 triggers proteolytic processing of HsCep250 and results in splitting of the duplicate centrosome. Notably, TgCep250 is also proteolytically processed and provides another parallel across

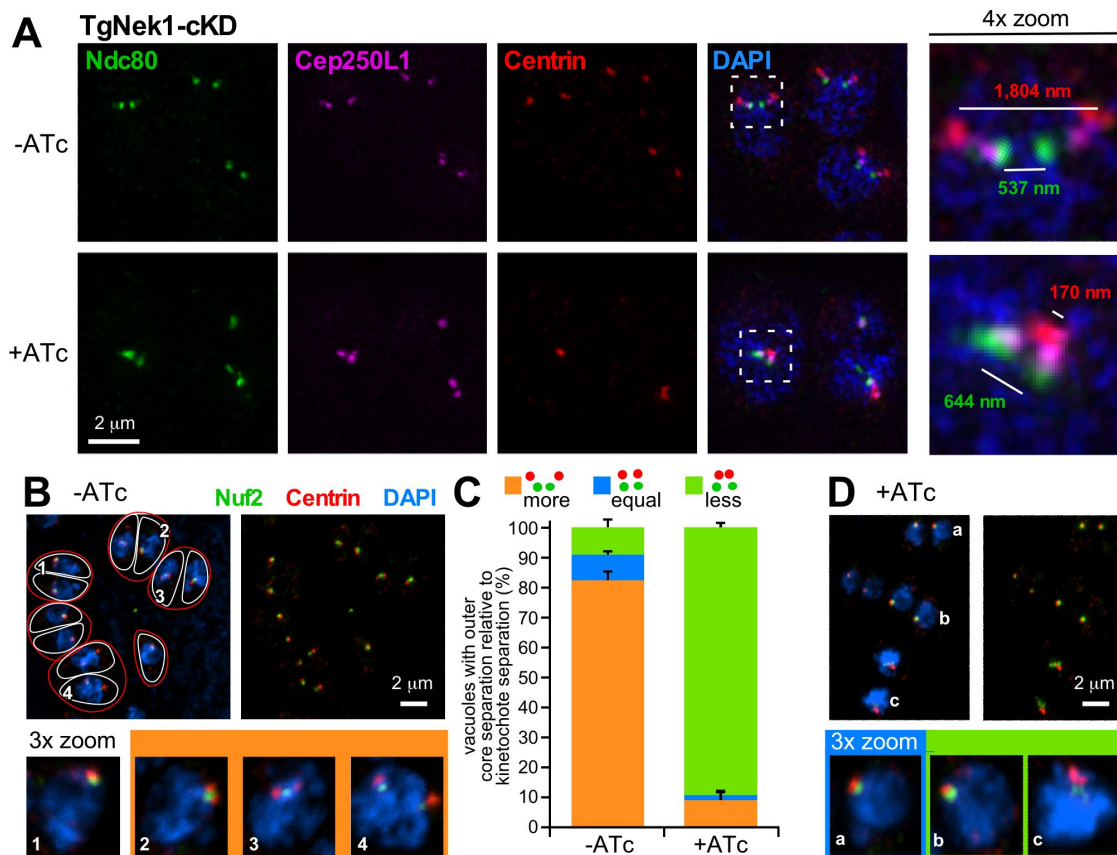


FIGURE 7: Loss of TgNek1 prevents outer core splitting but does not interfere with inner core separation. (A) Image acquired by superresolution microscopy (SIM) of TgNek1-cKD parasites \pm ATc for 18 h using kinetochore (α -Ndc80), centrosomal inner core (α -HA marking Cep250L1-HA), and outer core (α -Centrin) markers. Boxed areas magnified on the right. (B–D) Quantification of the relative level of kinetochore (Nuf2 antiserum) vs. outer core (TgCentrin1 antiserum) separation in TgNek1-cKD parasites grown \pm ATc for 18 h. (B) Representative phenotypes observed in normal (–ATc) parasites. Vacuoles are outlined in red; parasites in white. The numbered nuclei are magnified in the bottom panel and represent the sequential progression of centrosomal splitting coupled to mitosis. (C) Plot of quantification of phenotypes boxed in corresponding colors in B and D for relative separation of the kinetochores vs. the centrosomal outer cores. The definition of “more,” “equal,” and “less” outer core (red dots) separation relative to kinetochore (green dots) separation is defined in the little schematics in the legend. At least 100 vacuoles with duplicated kinetochore/centrosome pairs per condition and experiment were counted; error bars represent SD from three independent experiments. (D) Representative phenotypes observed in induced (+ATc) parasites; “a” to “c” mark nuclei enlarged in the bottom panels to represent the spectrum of scored phenotypes.

species. However, we do not know the exact function of TgCep250 in *Toxoplasma*, but we do know it is associated with the outer core at the onset of cytokinesis. It is tempting to speculate this could be related to activation of the outer core toward cytokinesis, or alternatively, it could be a step in centrosomal maturation. This question cannot be answered in *Toxoplasma* tachyzoites, as every mitotic round is connected with daughter budding.

In mammalian cells, the differential decoration of centriolar appendages defines the difference in age and ability to nucleate microtubules between the centriolar pairs (Bornens and Gonczy, 2014). *Toxoplasma*'s annotated genome does not contain orthologues of mammalian centriolar appendage genes, and no clear appendage structure was observed with transmission electron microscopy. Functionally, however, differential states of mother and daughter centrosomes have been postulated to originate the nongeometric daughter expansion numbers observed during schizogony in the *Plasmodium* spp. red blood cell cycle (Arnot *et al.*, 2011). In the proposed model, the mother centrosome is ready for another round of duplication, associated with S phase and mitosis, sooner than the daughter

centrosome, which still has to mature, and this is the mechanistic basis for nongeometric daughter numbers (Arnot *et al.*, 2011). In direct support of this model is our observation that the detachment of outer and inner cores occurs mostly in one pair of centrosomes upon Tg-Cep250 depletion. We show that TgCep250 is retained in the intact centrosome (mother) but is depleted from the destabilized daughter centrosome (Supplemental Figure S1). Our results therefore provide the first experimental evidence that daughter and mother centrosomes are different in apicomplexan parasites.

Overduplication of outer cores has been reported in parasites expressing a temperature-sensitive allele of the peripheral centrosomal matrix (PCM) component MAPK-L1 (Suvorova *et al.*, 2015), whereas outer core fragmentation was observed in TgCep530-depleted parasites (TgCep530 resides in between the inner and outer cores) (Courjol and Gissot, 2018). In TgCep250-depleted cells, we observed multiple outer cores, which could be the result of either overduplication or fragmentation (Figure 4, D and E). The TgCep250 phenotypes differs from the MAPK-L1-defective cells, as an accumulation of inner and outer cores aligned in a “dumbbell form”

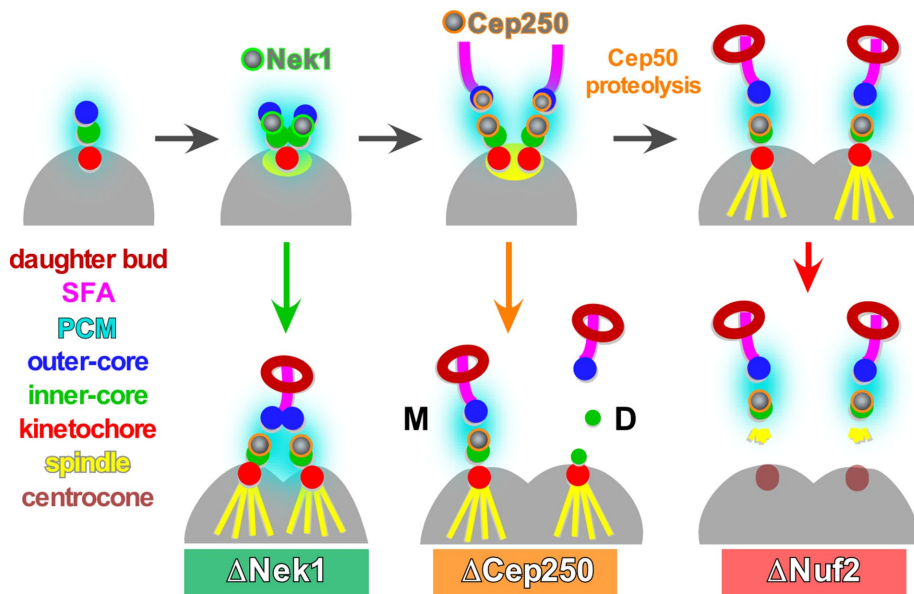


FIGURE 8: Schematic summarizing the spatiotemporal roles of TgCep250, TgNuf2, and TgNek1 throughout centrosomal replication, mitosis, and onset of daughter budding. Top sequence represents normal development, with the appearance of Nek1 and Cep250 specifically indicated. Note that Nek1 and Cep250 do not overlap in timing or location, thus making it unlikely Cep250 is a Nek1 substrate. Bottom schema represent the phenotypes upon depletion of the factors as labeled at the bottom. Note that Cep250 is retained on the mother (M) centrosome in the Cep250 knockdown line but results in a destabilized daughter (D) centrosome. For simplicity, daughter bud formation is represented by the appearance of ISP1 (see Figure 5E). SFA, striated fiber assembly; PCM, peripheral centrosomal matrix.

was not observed. On the other hand, the TgCep250 phenotype is also dramatically different from the multiple outer cores of various intensity observed in TgCep530-deficient parasites. The multiple outer cores observed upon TgCep250 depletion appear clearly organized and are of equal intensity, which is more consistent with an overduplication than with fragmentation. In addition, we observed normal initiation of daughter buds in the absence of TgCep250 (Figures 5, E and F, and 8), suggestive of fully functional outer cores.

This observation provides further support for the hypothesis of independent function and regulation of inner and outer cores as the basis to uncouple mitosis from daughter budding throughout the different multiplication strategies in the Apicomplexa (Chen and Gubbels, 2015; Suvorova *et al.*, 2015). In addition, the formation of spindle microtubules on disconnected inner cores (Figures 5, A and B, and 8) is also in line with the independent functionality of the bi-functional centrosomal cores. Further support for this model is provided in the IFA assay combining SFA, Centrin, TgCep250L1, and TgNdc80 (Figure 5, F and G), as the integrity of each of these structures appears normal, which is essential and critical for the endowment of each daughter cell with a single copy of genetic material (Beck *et al.*, 2010; Francia and Striepen, 2014). Indeed, we observed a hierarchical organization of these critical structures in wild-type parasites (Figure 5F). However, in TgCep250-cKD cells, the connection between the inner (green) and outer core (blue) is lost, while association between the SFA and outer core, as well as between the kinetochore and the inner core, remains intact (Figure 8). Taken together, our data are consistent with the previously hypothesized model of independent regulation of inner and outer cores in the bipartite centrosome (Suvorova *et al.*, 2015).

Our previous work showed that the kinetochore is required for outer core association with the nucleus (Farrell and Gubbels, 2014),

because it locks the microtubules emanating from the centrosome onto the nuclear envelope (Chen *et al.*, 2015). Using the novel tools developed here, we now expanded these insights by showing that, in TgNuf2-cKD parasites, the intact inner and outer core pair dissociates in its entirety from the nucleus (Figure 6). Thus, we can conclude that the kinetochore serves as a molecular anchor to lock the intact bipartite centrosome and that spindle microtubules anchoring to the nuclear periphery are not required to maintain the connection between the inner and outer cores.

Overall, we conclude that the centrosomal outer core, inner core, and kinetochore are hierarchically organized and that TgCep250 is essential for structural stability of the connection between the centrosomal cores embedded at the time of centrosomal duplication. Two different forms of Cep250 are present in tachyzoites: a full-length form localizing to the outer core during the transition between mitosis and cytokinesis and a proteolytically processed form localizing to the inner core throughout the tachyzoite cell cycle. It is unlikely that TgNek1 is the kinase triggering proteolytic cleavage. The tethering function of TgCep250 appears to be maintained between human and *Toxoplasma* orthologues, but the structures con-

nected are tailored to each organism. The phosphorylation controls and the proteolytic mechanisms in *Toxoplasma* remain unknown, but provide an exciting area for future research.

MATERIALS AND METHODS

Parasite strains

Toxoplasma gondii tachyzoites of RHΔHX (Donald and Roos, 1998), RHΔKu80ΔHX (Huynh and Carruthers, 2009), TATIΔKu80 (Sheiner *et al.*, 2011), and their transgenic derivatives were grown in human foreskin fibroblast as previously described (Roos *et al.*, 1994). Pyrimethamine (1 μM), chloramphenicol (20 μM), or mycophenolic acid (25 μg/ml) in combination with 50 μg/ml xanthine was used to select stable transgenic parasite lines and cloned by serial dilution. We used 1.0 μg/ml anhydrotetracycline to repress specific gene expression of conditional knockdown lines. Cep250Like-HA fosmid was kindly provided by Michael White, University of South Florida (Vinayak *et al.*, 2014). The *tub-EB1-YFP/sagCAT* plasmid has been described before (Chen *et al.*, 2015).

Plasmid constructs

All primers used are listed in Supplemental Table S1. Endogenously tagged parasite strains were generated as previously described (Sheiner *et al.*, 2011). Briefly, 1- and 1.9-kb regions upstream of the stop codon of the *TgCep250* gene were PCR amplified using genomic DNA from the *Toxoplasma* RH strain as a template and were cloned by ligation-independent cloning (LIC) into pYFP-LIC-DHFR (kindly provided by Vern Carruthers, University of Michigan). *NarI* was used to linearize pCep250-YFP-LIC-DHFR for site-specific homologous recombination.

Tetracycline-regulatable parasite strains were generated by single-crossover homologous recombination using a plasmid kindly

provided by Wassim Daher, University of Montpellier, France (Morton-Guyot *et al.*, 2014). The plasmid was redesigned by adding a single Myc-tag between the minimum promoter and the N-terminal genomic region of the target genes. All the inserts were amplified by PCR and digested with the enzyme pairs *Bgl*II and *Not*I. For construction of the Myc-Cep250-cKD line, the 5' end of the TgCep250 was amplified, digested with the *Bgl*II and *Not*I enzyme pairs, and ligated into the DHFR-TetO7sag4-Myc vector. The resulting construct was linearized using *Nco*I, electroporated into the TATIΔKu80 line by electroporation, and selected for pyrimethamine resistance. The Myc-Nek1-cKD line was generated following the same strategy.

The Myc-Cep250-3xTy-cKD line was generated by site-specific insertion of a PCR product carrying the tag and an HXGPRT selectable marker using CRISPR/Cas9. The pU6 plasmid expressing the guide RNA and Cas9 nuclease was kindly provided by Sebastian Lourido from the Whitehead Institute (Sidik *et al.*, 2014). The CRISPR construct targeted the 3'UTR of TgCep250 near the stop codon. A primer pair was designed to amplify the 3xTy tag and the selectable marker (HXGPRT) flanking it with 40 base pairs of homologous region before the stop codon and after the protospacer-adjacent motif site. Amplicon generated from the primer pair was gel purified and cotransfected with the protospacer and Cas9 encoding plasmid.

IFA and microscopy

Parasites were seeded overnight (~16–18 h) and fixed with methanol as previously described (Gubbels *et al.*, 2006). The following antibodies were used in this study: Myc (MAb 9E10, mouse, 1:50; Santa Cruz); HA (3F10, rat, 1:3000; Roche); TgIMC3 (rat, 1:2000; Anderson-White *et al.*, 2011); TgNuf2 and TgNdc80 (guinea pig, 1:2000; Farrell and Gubbels, 2014); SFA (rabbit, 1:1000; kindly provided by Boris Striepen, University of Georgia; Francia *et al.*, 2012); TgNek1 (1:1000; Chen and Gubbels, 2013); HsCentrin (rabbit, 1:1000; kindly provided by Iain Cheeseman, Whitehead Institute); Ty (mouse, 1:1000; kindly provided by Sebastian Lourido); TgEB1 (rat, 1:3000; this work). Alexa Fluor A488, A568, A594, A633, and A647 secondary antibodies were used. We used 4',6'-diamidino-2-phenylindole (DAPI) to stain nuclear material. Images were acquired using a Zeiss Axiovert 200M wide-field fluorescence microscope equipped with a Plan-Fluor 100x/1.45 NA oil objective and a Hamamatsu Orca-Flash 4.0LT camera. For superresolution structured illumination microscopy (SIM), a Zeiss Elyra S.1 microscope equipped with a Plan-Apochromat 63x/1.40 oil objective and a PCO-Tech pco.edge 4.2 sCMOS camera in the Boston College Imaging Core was used in consultation with Bret Judson. Images were acquired and processed in Zeiss ZEN v. 2.3 software using the standard mode.

EB1 antiserum generation

For generation of N-terminal His₆-tagged fusion protein, 600 base pairs from TgEB1 cDNA (corresponding to the N-terminal 200 amino acids) were PCR amplified using primers EB1-(F/R)-LIC-His and cloned into the pAVA0421 plasmid (Alexandrov *et al.*, 2004) by ligation-independent cloning. The fusion protein was expressed in BL21 STAR (DE3)pLysS *Escherichia coli* using 0.5 mM isopropyl β-D-1-thiogalactopyranoside in 2xYT broth overnight at 37°C and purified under native conditions over Ni-NTA agarose (Invitrogen). Polyclonal antiserum was generated by immunization of a rat (Covance, Denver, PA). Antisera were affinity purified as previously described (Gubbels *et al.*, 2006) against recombinant His₆-TgEB1.

Western blot analysis

Freshly lysed parasites were collected after 3-μm filtration by centrifugation and washed twice in 1X phosphate-buffered saline. Parasite

pellets were lysed by resuspension in 50 mM Tris-HCl (pH 7.8), 150 mM NaCl, and 1% SDS containing 1X protease inhibitor cocktail (Sigma-Aldrich) and heating at 95°C for 10 min. Parasite lysates were analyzed by SDS-PAGE on a 3–8% Tris-acetate gradient gel. Before polyvinylidene fluoride membrane transfer, the gel was subjected to 100 mM acetic acid for 5 h to break up the large TgCep250 protein. Transfer buffer contained 25 mM Tris (pH 8.3), 195 mM glycine, 0.025% (wt/vol) SDS, and 15% methanol. Blots were hybridized with α-Myc-HRP, α-Ty, or α-α-tubulin (MAb 12G10; Developmental Studies Hybridoma Bank).

ACKNOWLEDGMENTS

We thank William Jacobus and Emily Stoneburner for technical assistance and V. Carruthers, I. Cheeseman, W. Daher, S. Lourido, B. Striepen, E. Suvorova, and M. White and for sharing reagents. We thank Bret Judson and the Boston College Imaging Core for infrastructure and support and M. White and E. Suvorova for fruitful suggestions and discussion. This study was supported by National Science Foundation major instrumentation grant 1626072 and through support from National Institutes of Health grants AI110690, AI110638, and AI128136.

REFERENCES

- Agircan FG, Schiebel E, Mardin BR (2014). Separate to operate: control of centrosome positioning and separation. *Philos Trans R Soc Lond B Biol Sci* 369, 20130461.
- Alexandrov A, Vignali M, LaCount DJ, Quartley E, de Vries C, De Rosa D, Babulski J, Mitchell SF, Schoenfeld LW, Fields S, *et al.* (2004). A facile method for high-throughput co-expression of protein pairs. *Mol Cell Proteomics* 3, 934–938.
- Alvarez CA, Suvorova ES (2017). Checkpoints of apicomplexan cell division identified in *Toxoplasma gondii*. *PLoS Pathog* 13, e1006483.
- Anderson-White BR, Beck JR, Chen CT, Meissner M, Bradley PJ, Gubbels MJ (2012). Cytoskeleton assembly in *Toxoplasma gondii* cell division. *Int Rev Cell Mol Biol* 298, 1–31.
- Anderson-White BR, Ivey FD, Cheng K, Szatanek T, Lorestani A, Beckers CJ, Ferguson DJ, Sahoo N, Gubbels MJ (2011). A family of intermediate filament-like proteins is sequentially assembled into the cytoskeleton of *Toxoplasma gondii*. *Cell Microbiol* 13, 18–31.
- Arnot DE, Ronander E, Bengtsson DC (2011). The progression of the intracellular cell cycle of *Plasmodium falciparum* and the role of the centriolar plaques in asynchronous mitotic division during schizogony. *Int J Parasitol* 41, 71–80.
- Bahe S, Stierhof YD, Wilkinson CJ, Leiss F, Nigg EA (2005). Rootletin forms centriole-associated filaments and functions in centrosome cohesion. *J Cell Biol* 171, 27–33.
- Beck JR, Rodriguez-Fernandez IA, Cruz de Leon J, Huynh MH, Carruthers VB, Morrisette NS, Bradley PJ (2010). A novel family of *Toxoplasma* IMC proteins displays a hierarchical organization and functions in coordinating parasite division. *PLoS Pathog* 6, e1001094.
- Bornens M, Gonczy P (2014). Centrosomes back in the limelight. *Philos Trans R Soc Lond B Biol Sci* 369.
- Brooks CF, Francia ME, Gissot M, Croken MM, Kim K, Striepen B (2011). *Toxoplasma gondii* sequesters centromeres to a specific nuclear region throughout the cell cycle. *Proc Natl Acad Sci USA* 108, 3767–3772.
- Chen CT, Gubbels MJ (2013). The *Toxoplasma gondii* centrosome is the platform for internal daughter budding as revealed by a Nek1 kinase mutant. *J Cell Sci* 126, 3344–3355.
- Chen CT, Gubbels MJ (2015). Apicomplexan cell cycle flexibility: centrosome controls the clutch. *Trends Parasitol* 31, 229–230.
- Chen CT, Kelly M, Leon J, Nwagbara B, Ebbert P, Ferguson DJ, Lowery LA, Morrisette N, Gubbels MJ (2015). Compartmentalized *Toxoplasma* EB1 bundles spindle microtubules to secure accurate chromosome segregation. *Mol Biol Cell* 26, 4562–4576.
- Courjol F, Gissot M (2018). A coiled-coil protein is required for coordination of karyokinesis and cytokinesis in *Toxoplasma gondii*. *Cell Microbiol* 20, e12832.
- Donald RG, Roos DS (1998). Gene knock-outs and allelic replacements in *Toxoplasma gondii*: HXGPRT as a selectable marker for hit-and-run mutagenesis. *Mol Biochem Parasitol* 91, 295–305.
- Farrell M, Gubbels MJ (2014). The *Toxoplasma gondii* kinetochore is required for centrosome association with the centrocone (spindle pole). *Cell Microbiol* 16, 78–94.

- Ferguson DJ, Hutchison WM, Dunachie JF, Siim JC (1974). Ultrastructural study of early stages of asexual multiplication and microgametogony of *Toxoplasma gondii* in the small intestine of the cat. *Acta Pathol Microbiol Scand B Microbiol Immunol* 82, 167–181.
- Francia ME, Jordan CN, Patel JD, Sheiner L, Demerly JL, Fellows JD, de Leon JC, Morrissette NS, Dubremetz JF, Striepen B (2012). Cell division in Apicomplexan parasites is organized by a homolog of the striated rootlet fiber of algal flagella. *PLoS Biol* 10, e1001444.
- Francia ME, Striepen B (2014). Cell division in apicomplexan parasites. *Nat Rev Microbiol* 12, 125–136.
- Fry AM, Mayor T, Meraldi P, Stierhof YD, Tanaka K, Nigg EA (1998). C-Nap1, a novel centrosomal coiled-coil protein and candidate substrate of the cell cycle-regulated protein kinase Nek2. *J Cell Biol* 141, 1563–1574.
- Gubbels MJ, Vaishnav S, Boot N, Dubremetz JF, Striepen B (2006). A MORN-repeat protein is a dynamic component of the *Toxoplasma gondii* cell division apparatus. *J Cell Sci* 119, 2236–2245.
- Gubbels MJ, White M, Szatanek T (2008). The cell cycle and *Toxoplasma gondii* cell division: tightly knit or loosely stitched? *Int J Parasitol* 38, 1343–1358.
- He R, Huang N, Bao Y, Zhou H, Teng J, Chen J (2013). LRRC45 is a centrosome linker component required for centrosome cohesion. *Cell Rep* 4, 1100–1107.
- Huynh MH, Carruthers VB (2009). Tagging of endogenous genes in a *Toxoplasma gondii* strain lacking Ku80. *Eukaryot Cell* 8, 530–539.
- Morlon-Guyot J, Berry L, Chen CT, Gubbels MJ, Lebrun M, Daher W (2014). The *Toxoplasma gondii* calcium dependent protein kinase 7 is involved in early steps of parasite division and is crucial for parasite survival. *Cell Microbiol* 16, 95–114.
- Morlon-Guyot J, Francia ME, Dubremetz JF, Daher W (2017). Towards a molecular architecture of the centrosome in *Toxoplasma gondii*. *Cytoskeleton (Hoboken)* 74, 55–71.
- Nishi M, Hu K, Murray JM, Roos DS (2008). Organellar dynamics during the cell cycle of *Toxoplasma gondii*. *J Cell Sci* 121, 1559–1568.
- Roos DS, Donald RG, Morrissette NS, Moulton AL (1994). Molecular tools for genetic dissection of the protozoan parasite *Toxoplasma gondii*. *Methods Cell Biol* 45, 27–63.
- Sheiner L, Demerly JL, Poulsen N, Beatty WL, Lucas O, Behnke MS, White MW, Striepen B (2011). A systematic screen to discover and analyze apicoplast proteins identifies a conserved and essential protein import factor. *PLoS Pathog* 7, e1002392.
- Sidik SM, Hackett CG, Tran F, Westwood NJ, Lourido S (2014). Efficient genome engineering of *Toxoplasma gondii* using CRISPR/Cas9. *PLoS One* 9, e100450.
- Suvorova ES, Francia M, Striepen B, White MW (2015). A novel bipartite centrosome coordinates the apicomplexan cell cycle. *PLoS Biol* 13, e1002093.
- Trecek M, Sanders JL, Elias JE, Boothroyd JC (2011). The phosphoproteomes of *Plasmodium falciparum* and *Toxoplasma gondii* reveal unusual adaptations within and beyond the parasites' boundaries. *Cell Host Microbe* 10, 410–419.
- Vinayak S, Brooks CF, Naumov A, Suvorova ES, White MW, Striepen B (2014). Genetic manipulation of the *Toxoplasma gondii* genome by fosmid recombineering. *MBio* 5, e02021.